

Statistical fluxes and the Curie-Weiss metal state

Kai Wu,¹ Zheng-Yu Weng,¹ and Jan Zaanen²¹*Institute for Advanced Study, Tsinghua University, Beijing, 100084, China*²*Instituut Lorentz for Theoretical Physics, Leiden University, Leiden, P.O. Box 9506, 2300 RA Leiden, The Netherlands*

(Received 5 September 2011; published 30 September 2011)

We predict a new state of matter in the triangular t - J model in a high doping regime. Due to the altered role of quantum statistics the spins are “localized” in statistical Landau orbits, while the charge carriers form a Bose metal that feels the spins through random gauge fields. In contrast to the Fermi-liquid state, this state naturally exhibits a Curie-Weiss susceptibility, large thermopower, and linear-temperature resistivity, explaining the physics of Na_xCoO_2 at $x > 0.5$. A “smoking gun” prediction for neutron scattering is presented.

DOI: [10.1103/PhysRevB.84.113113](https://doi.org/10.1103/PhysRevB.84.113113)

PACS number(s): 71.10.Hf, 71.27.+a, 72.80.Ga

Introduction. Among the great challenges in quantum matter physics is the question whether Mottness—the drastic change of Hilbert space structure due to strong local interactions—might form the condition for non-Fermi liquid states of fermionic matter to occur.^{1,2} Among others, this is the point of departure of Anderson’s resonating valence bond (RVB) proposal for high- T_c superconductivity.³ At the electron densities in the proximity of the half-filled Mott insulator, the Mott projections are most evident and it is much less evident whether they matter at all at very high (or dilute) electron densities. Resting on a representation^{2,4} that makes explicit the altered nature of the quantum statistics due to Mottness, we demonstrate here the existence of an internally consistent, stable saddle point at high dopings on a triangular lattice. This is a spin-charge separated state where the doublons (carrying charge) and spinons (carrying spin) are coded as hard core bosons that communicate with each other via statistical fluxes. The surprise is in the spin sector: the statistical gauge fields act like a uniform magnetic field causing Landau quantization of the spinon states. The spinons are localized in Landau orbits of the lowest Landau level (LLL) at low temperatures, with the effect that these behave as free Curie-Weiss spins with large entropy. The doublons get in turn scattered by the random gauge fluxes associated with the localized spinons, similarly as in gauge glass models.

This might sound far fetched. However, the microscopy matches that of the highly overdoped Na_xCoO_2 system^{5–7} with $x > 0.5$. A very strange metal is formed in this cobaltate, characterized by a high density of free Curie-Weiss spins that “appear out of the blue” while it is a rather good hole-type thermoelectric material⁸ given its large thermopower combined with a relatively low resistivity. We will show here that the magnetic (Fig. 1), thermoelectric (Fig. 2), and resistive (Fig. 3) properties of the cobaltate are consistent with the state described in the previous paragraph. We notice that earlier attempts^{9–14} also have potentially explained the aforementioned Curie-Weiss metal behavior of the cobaltates by invoking a very small bandwidth or strong disorder localization, however we present a smoking gun prediction that can be straightforwardly tested by experiment: the spin excitation spectrum should carry the fingerprints of the “spontaneous” Landau quantization (Fig. 4).

Similar to the layered structure in the high- T_c cuprates, the CoO_2 layer is believed to play an essential role in determining the low-energy physics in the Na_xCoO_2 compound. With

electrons doping introduced by Na, the electron hopping at the partially filled t_{2g} orbitals of the Co^{+3} ions and spin correlations between Co^{+4} ions in a CoO_2 layer may be minimally described by the t - J model^{15–17} on a triangular lattice with hopping amplitude $t < 0$.^{18–20} Here the Hilbert space is constrained by $\sum_{\sigma} c_{i\sigma}^{\dagger} c_{i\sigma} \geq 1$, that is, each lattice site is either singly occupied by an electron (Co^{+4}) or doubly occupied by electrons (Co^{+3}) without allowing the empty site (Co^{+5}). What we will be interested in is the highly overdoped regime of this model, where the RVB^{15–17} correlations induced by the superexchange coupling disappear and the hopping processes of both charge and spin become dominant.

Sign structure. To identify the new saddle point, we have to rely on a particular representation that is superficially reminiscent of the standard slave bosons but is actually quite different. This “phase string” representation^{2,4} is making explicit the non-Fermi-Dirac nature of the quantum statistics in doped Mott insulators. According to this formalism, the electron operator $c_{i\sigma}$ can be fully “bosonized” by $c_{i\sigma}^{\dagger} = d_i^{\dagger} b_{i-\sigma} e^{-i\Theta_{i\sigma}^{\text{string}}}$, where the doublon and spinon creation operators d_i^{\dagger} and $b_{i\sigma}^{\dagger}$ are both *bosonic*, which satisfy an equality (Mott) constraint $n_i^d + \sum_{\sigma} n_{i\sigma}^b = 1$ with n_i^d and $n_{i\sigma}^b$ denoting the doublon and spinon occupation numbers, respectively. Here the fermionic commutations of the electron operators are ensured by the topological phase $\Theta_{i\sigma}^{\text{string}} \equiv [\Phi_i^{\sigma} + \sigma \Phi_i^d]/2$, with $\Phi_i^{\sigma} \equiv \sum_{l \neq i} \theta_i(l) \sum_{\sigma} \sigma n_{l\sigma}^b$ and $\Phi_i^d \equiv \sum_{l \neq i} \theta_i(l)(1 - n_l^d)$, where $\theta_i(l) = \text{Im}(z_l - z_i)$ (z_i is the complex coordinate of site i). In this representation, the hopping and superexchange terms of the t - J model become

$$H_t = t \sum_{(ij)\sigma} \hat{D}_{ji} \hat{B}_{ij}^{\sigma} + \text{H.c.}, \quad (1)$$

$$H_J = -\frac{J}{2} \sum_{(ij)\sigma} \hat{B}_{ij}^{\sigma} \hat{B}_{ji}^{-\sigma} - \frac{J}{2} \sum_{(ij)\sigma} n_{i\sigma}^b n_{j-\sigma}^b, \quad (2)$$

in terms of $\hat{D}_{ij} \equiv e^{iA_{ij}^s} d_i^{\dagger} d_j$ and $\hat{B}_{ij}^{\sigma} \equiv e^{-i\sigma A_{ij}^d} b_{i\sigma}^{\dagger} b_{j\sigma}$. In this way, the remnant sign structure after Mott projection has been made explicit while it is precisely represented by the topological link variables A_{ij}^s and A_{ij}^d . Obviously there would

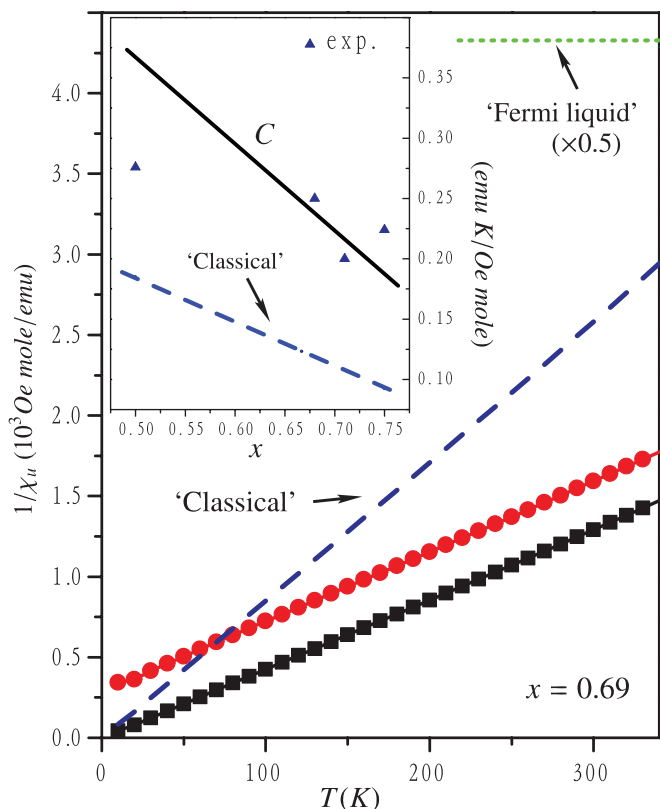


FIG. 1. (Color online) The spin part of the present electron fractionalization state exhibits a Curie T -dependent uniform susceptibility $\chi_u = C/T$ (full squares) at $x = 0.69$. The Weiss term in χ_u appears as an RPA correction (full circles). The Fermi liquid (dotted) and classical limit (dashed) results are also shown for comparison. Inset: the coefficient C (solid) and the classical limit C_{cl} (dashed) vs doping x , in which the experimental data are marked by full triangles.^{7,22,23}

be no “sign problem” should $A_{ij}^s = A_{ij}^d = 0$ in such a fully bosonized model with $t < 0$. Here A_{ij}^s and A_{ij}^d satisfy

$$\sum_{(ij) \in \partial S} A_{ij}^s = \pi \sum_{l \in S} \sum_{\sigma} \sigma n_{l\sigma}^b, \quad (3)$$

$$\sum_{(ij) \in \partial S} A_{ij}^d = \pi \sum_{l \in S} (1 - n_l^d), \quad (4)$$

where ∂S denotes the boundary of an area S .

Electron fractionalization saddle point. The precise sign structure identified above will be crucial in constructing the following saddle point which respects the gauge invariance associated with A_{ij}^s and A_{ij}^d , together with time reversal and spin rotational symmetries. Since the RVB pairing is irrelevant at high doping, the gauge-invariant \hat{D}_{ij} and \hat{B}_{ij}^{σ} in Eqs. (1) and (2) will be natural order parameters, resulting in an effective $H_{\text{eff}} = H_d + H_s$:

$$H_d = -t_d \sum_{(ij)} e^{-ia_{ij}} (e^{iA_{ij}^s} d_i^{\dagger} d_j) + \text{H.c.}, \quad (5)$$

$$H_s = -t_s \sum_{(ij)\sigma} e^{-ia_{ij}} (e^{-i\sigma A_{ij}^d} b_{i\sigma}^{\dagger} b_{j\sigma}) + \text{H.c.}, \quad (6)$$

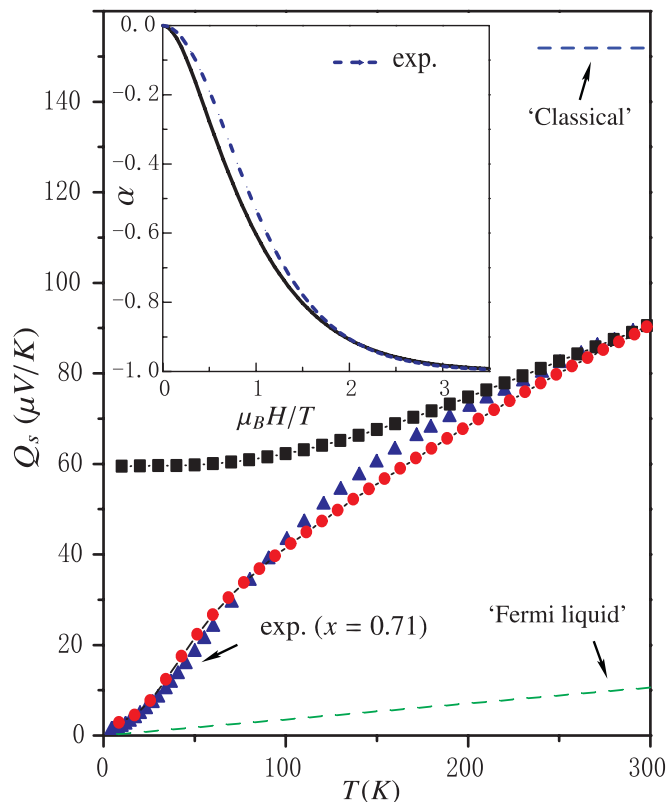


FIG. 2. (Color online) Thermopower Q_s contributed by the spin part at $x = 0.71$. Full squares: the mean-field solution; Full circles: the effect of doublon density fluctuations is considered (see text). The experimental result (full triangles) at the same x as well as the Fermi liquid (dotted) and “classical limit” (dashed) results are shown for comparison. Inset: The scaling curve (solid) for α defined in Eq. (7) vs H/T and the spin-entropy of free moments (dashed), which well accounts for the experiment measurement.⁶

where $t_d = -tB > 0$, $t_s = -tD + JB/4 > 0$. Here a_{ij} represents the $U(1)$ gauge fluctuations around the saddle point: $\hat{D}_{ij} \simeq D e^{ia_{ij}}$ and $\hat{B}_{ij}^{\sigma} \simeq (B/2) e^{ia_{ij}}$ which will recombine spins and charges together to electrons and destroy the mean-field saddle point. It can be shown²¹ that the saddle-point state is stable against the *transverse* fluctuations of a_{ij} , implying spin-charge separation. One simple way to see it is to note that the longitudinal component of a_{ij} will reinforce the Mott constraint relaxed at the saddle-point level. Under such a constraint, the topological condition (4) may be replaced by $\sum_{(ij) \in \partial S} A_{ij}^d = \pi \sum_{l \in S} \sum_{\sigma} n_{l\sigma}^b$, which means H_s in (6) actually describes a two-component (with spin index σ) *semionic* system. (The spin index σ before A_{ij}^d actually guarantees the time reversal symmetry.) More detailed discussion will be presented elsewhere²¹ and in the following we shall focus on the saddle point at $a_{ij} = 0$ in (5) and (6). As the phase string theory in the underdoped regime, this saddle point does not break any symmetries such as the time-reversal symmetry and spin rotation symmetry.⁴

Mean-field approximation. The spin dynamics is governed by H_s , where A_{ij}^d given in Eq. (4) is only density dependent and can therefore, to leading order approximation, be treated

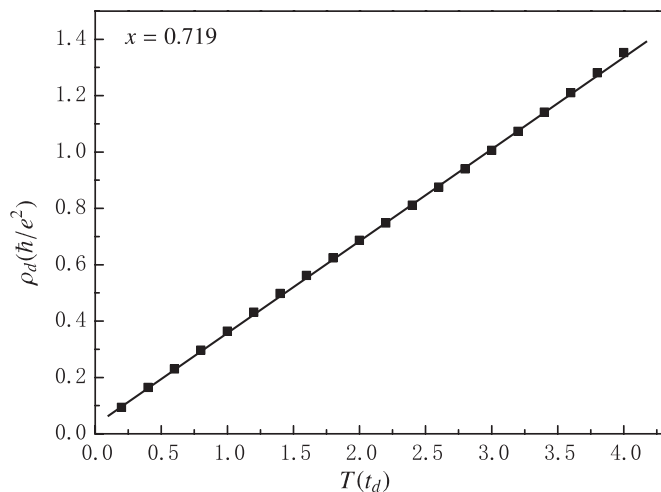


FIG. 3. The resistivity is contributed by doublons in the presence of random flux tubes $\pm\pi$ attached to spinons in the LLLs, which numerically treated as a random distribution of $\pm(1-\delta)\pi$ fluxes per unit cell.

as a smearing flux of $\pi(1-x)$ per unit cell. The resulting mean-field state of H_s is Landau quantized with spins being statistically localized in the cyclotron orbits, in sharp contrast with a degenerate Fermi liquid state or a fully localized classical state at $t \rightarrow 0$. In particular, the characteristic bandwidth vanishes, while t remains relatively large, when all the spinons stay in the degenerate LLLs at low temperatures, rendering a systematic scaling behavior as will be shown below.

Curie-Weiss uniform susceptibility. One peculiar property is exhibited by the uniform spin susceptibility, $\chi_u = \frac{2\mu_B^2\beta}{N} \sum_m (n_m + 1)n_m$ where $\beta^{-1} = k_B T$ and $n_m = 1/[e^{\beta(E_m - \mu_s)} - 1]$ is the Bose distribution for spinons at state m with energy E_m obtained by the aforementioned mean-field solution based on H_s (μ_s is the chemical potential). As clearly illustrated in Fig. 1 by $1/\chi_u$, it follows a Curie-Weiss law $\chi_u = \frac{C}{T + \Theta}$ with $\Theta = 0$ (full squares). A finite Weiss term $\Theta \simeq 3(1-x)J/k_B$ (full circles) is generated by including an RPA correction from H_J (by fitting with the experimental Θ ,⁶ we estimate $J \simeq 70$ K). The coefficient C is x dependent, and at $T \rightarrow 0$ one finds $C = 2(1-x)\mu_B^2/k_B$. As shown in the inset of Fig. 1, C is in quantitative agreement with the experimental data^{7,22,23} in the Curie-Weiss regime of the cobaltates, which is independent of other parameters in the model, like t and J .

By contrast, a Pauli-like susceptibility is expected for the Fermi-liquid state (dotted line in Fig. 1, obtained with a bare $t = -0.1$ eV²⁴). It is particularly instructive to compare this with the classical limit of the t - J model at $t \rightarrow 0$ ($J = 0$), where all the electrons are fully localized as $(1-x)N$ free moments, contributing to a Curie's law $\chi_u^{\text{cl}} = C_{\text{cl}}/T$ (dashed line in Fig. 1). But one finds $C_{\text{cl}} = C/2$, that is, only about the *half* of the values of both the experimental and the present theory (cf. the inset of Fig. 1). Clearly the peculiar quantum effect of the present bosonic spinons is responsible for the enhancement of C from C_{cl} at low T (only at high- T limit, the "classical" χ_u^{cl} can be recovered as $n_m \rightarrow 0$ in χ_u).

Thermopower. In Fig. 2 the thermopowers predicted by the Fermi-liquid state as well as the classical limit of the t - J model are shown by dotted and dashed curves, respectively. In

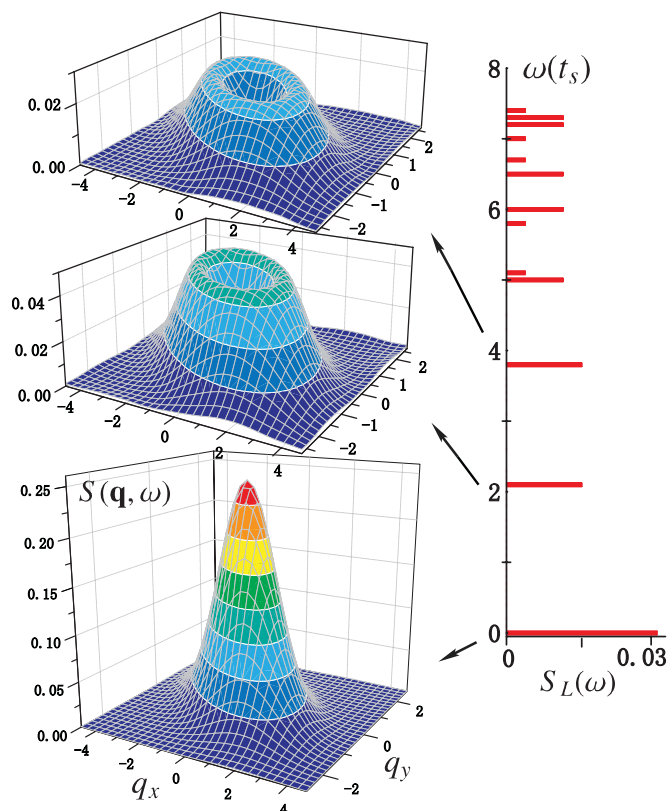


FIG. 4. (Color online) Dynamic spin structure factor $S(\mathbf{q}, \omega)$ predicted by the mean-field theory at $x = 0.75$. Right panel: the Landau level structure exhibited in the local (\mathbf{q} -integrated) dynamic structure factor $S_L(\omega)$. Left panel: the corresponding \mathbf{q} dependence of $S(\mathbf{q}, \omega)$ for the first three energy levels.

the latter case, with the bandwidth vanishing, the thermopower reduces to the so-called Heikes formula: $Q_{\text{cl}} = (k_B/e) \ln \frac{2x}{(1-x)}$ which is proportional to the entropy per electron.^{25,26} Both deviate strongly from the experimental result (full triangles in Fig. 2) in opposite ways.

In the present saddle-point state, the thermopower will satisfy the Ioffe-Larkin combination rule $Q = Q_d + Q_s$ according to Eqs. (5) and (6), with the spinon contribution Q_s dominant over the doublon part Q_d . Here a large Q_s originates in the degeneracy of the LLLs. This leads to a Heikes-like formula $Q_s = -\mu_s/eT$, associated with the spinon entropy, which follows given that the energy-particle current correlator $S^{12} = 0$ at low temperature in the Kubo formula $Q_s = -\frac{1}{eT} \frac{S^{12}}{S^{11}} - \frac{\mu_s}{eT}$.²⁷ Note that the above Heikes-like formula is still valid even when S^{12} becomes finite, for instance when the spinons are excited to the higher Landau levels at high T , because the current-current correlator $S^{11} \rightarrow \infty$.^{21,28-30}

The calculated Q_s is presented in Fig. 2 (solid squares). This saturates at low T to a universal value $Q_{s0} = \frac{k_B}{e} \ln 2 \approx 60$ $\mu\text{V}/\text{K}$ due to the artifact that the bandwidth of the LLLs remains zero. But a weak fluctuation of the gauge flux of A_{ij}^d around the mean value can easily cause a broadening, lifting the exact LLL degeneracy, resulting in a vanishing Q_s at $T \rightarrow 0$. A typical example is indicated by the full circles in Fig. 2, with A_{ij}^d simulated by a random flux of $[-0.3\pi, 0.3\pi]$

around the mean flux of $\pi(1-x)$ per unit cell. One finds a quantitative agreement with the experimental measurement by taking $t_s = 100$ K. Note that Q_d contributed by doublons is not included here as it is usually much weaker in magnitude with a quite flat T dependent as calculated by the Kubo formula.²¹

To understand more clearly the origin of Q_s from the spin degrees of freedom, one may apply a strong in-plane magnetic field H to polarize (freeze) the spins via Zeeman energy, as already accomplished experimentally.⁶ Denote $Q_s(\infty)$ as the contribution from the remaining configurational entropy at $H \rightarrow \infty$ and define

$$\alpha = \frac{Q_s(H) - Q_s(\infty)}{Q_s(0) - Q_s(\infty)} - 1. \quad (7)$$

Then α is found to be a well-defined scaling curve of H/T , as shown by the solid curve in the inset of Fig. 2, which fits well with the pure spin entropy of free moments: $[\ln[2 \cosh(u)] - u \tanh(u)] / \ln 2$, where $u = (2.2\mu_B H) / (2k_B T)$ in excellent agreement with the experimental data as given in Ref. 6.

Resistivity. The resistivity satisfies the Ioffe-Larkin combination rule $\rho = \rho_d + \rho_s$ in which $\rho_s = 0$ due to the aforementioned ‘‘Meissner effect’’ response^{21,28–30} in the spinon subsystem such that the doublon subsystem will solely contribute to ρ . Governed by H_d , the doublons will experience the novel scattering generated from the gauge potential A_{ij}^s , which describes $\pm\pi$ flux tubes bound to the spinons with $\sigma = \pm$. In the low- T regime where the spinons are in the degenerate Landau orbits, the corresponding flux tubes seen by the holons will distribute randomly in space. Based on a numerical calculation where A_{ij}^s is treated as randomly distributed $\pm(1-x)\pi$ fluxes per unit cell, we obtain a metallic behavior of ρ_d with a linear- T dependence over a large temperature regime as shown in Fig. 3, originating in a scattering rate similar to a case previously studied³¹ in a high- T regime in the context of high- T_c cuprates.

Predictions and discussion. The fractionalized saddle-point state governed by (5) and (6) has been shown to generically exhibit a systematic scaling behavior: $\rho \propto T$, $\chi_u \propto 1/T$, a large thermopower $Q_s \sim \frac{k_B}{e} \ln 2$, as well as the scaling law in $\alpha = \alpha(H/T)$, associated with the peculiar Landau quantization effect in H_s . Our theory allows us to make one further strong prediction: the spin sector Landau levels can be in fact directly observed by inelastic neutron scattering! The dynamic spin structure factor $S(\mathbf{q}, \omega)$ can be easily computed assuming the straightforward Landau quantization and it should look like Fig. 4: a tower of rather narrow nondispersive bands of spin fluctuation (right panel), with a momentum dependence as indicated in the left panel.

Another interesting consequence of the spin-charge separation is in the figure of merit used to quantify the efficiency of a thermoelectric device. This can be written in the following

form:

$$ZT \equiv \frac{Q^2 T}{\rho \kappa} = \frac{(Q_s + Q_d)^2 / L_d}{1 + \kappa_{ph} / \kappa_d} \quad (8)$$

since the spinons do not contribute to the thermal conductivity and resistivity ($\kappa_s = 0$ and $\rho_s = 0$).²¹ Then a large spinon thermopower $Q_s (\gg |Q_d|)$ will play an important role, independent of the Lorenz number of the doublons $L_d \equiv \frac{T}{\kappa_d \rho_d}$ as well as the doublon (κ_d) and phonon (κ_{ph}) thermal conductivities. We find²¹ L_d to be one order of magnitude smaller than the Lorenz number of a Fermi liquid. This is in fact consistent with exact diagonalization result on the t - J model.³² The combination of these factors may therefore lead potentially to an exceptionally large Z .

Finally, we emphasize that in principle a sharp LLL degeneracy is an artifact of the mean-field approximation which can be easily lifted, for instance, by density fluctuations via A_{ij}^d intrinsically or extrinsically (e.g., induced by the distribution of Na),^{33–35} which leads to other stable phases at low temperature. Nonetheless, the mean-field results is expected to remain a good approximation to the saddle-point physics at ‘‘intermediate’’ temperatures higher than the LLL broadening. Namely, the physics we have discussed here is associated with an intermediate temperature regime, bounded by the Landau gap scale at high temperature and the onset of further cooperative phenomena at low temperatures. In the latter regime the specific heat measurements have also shown^{36,37} an anomalous increase, presumably due to the afore-discussed entropy enhancement which, however, will be sensitive to the detailed Landau level broadening. Eventually the spin degeneracies associated with the Landau states will be lifted, and this might be the origin of some new emergent orders at very low temperatures. One infers from the momentum dependence of $S(\mathbf{q}, \omega)$ at the LLLs (Fig. 4) that the in-plane ferromagnetic correlation length will increase with x , such that a small interlayer superexchange J_\perp may eventually drive an in-plane ferromagnetic order with antiferromagnetic ordering along different layers, explaining the A -type antiferromagnetic order observed by neutron scattering at $x \geq 3/4$.³⁸ The bosonic doublons may also condense at a sufficiently low T to make the system more Fermi-liquid like, reconciling with the Wiedemann-Franz law observed in $\text{Na}_{0.7}\text{CoO}_2$ at $T < 1$ K.³⁹ However our unconventional ‘‘building material’’ also leaves room for less conventional forms of order, including uncommon charge orders that will be discussed in detail elsewhere.

We acknowledge stimulating discussions with N. P. Ong, X. L. Qi, and in particular Y. Wang who also provided us with unpublished experimental data. This work was supported by the grants of NSFC and the National Program for Basic Research of MOST, China, and a Spinoza grant of the Nederlandse Organisatie voor Wetenschappelijk Onderzoek (NWO).

¹P. W. Anderson, *The Theory of Superconductivity in the High T_c Cuprates* (Princeton University Press, Princeton, 1997).

²J. Zaanen and B. J. Overbosch, e-print [arXiv:0911.0470](https://arxiv.org/abs/0911.0470).

³P. W. Anderson, *Science* **235**, 1196 (1987).

⁴Z.-Y. Weng, *Int. J. Mod. Phys. B* **21**, 773 (2007).

- ⁵I. Terasaki, Y. Sasago, and K. Uchinokura, *Phys. Rev. B* **56**, R12685 (1997).
- ⁶Y. Wang *et al.*, *Nature (London)* **423**, 425 (2003).
- ⁷M. L. Foo, Y. Wang, S. Watauchi, H. W. Zandbergen, T. He, R. J. Cava, and N. P. Ong, *Phys. Rev. Lett.* **92**, 247001 (2004).
- ⁸M. Lee *et al.*, *Nat. Mater.* **5**, 537 (2006).
- ⁹O. I. Motrunich and P. A. Lee, *Phys. Rev. B* **69**, 214516 (2004).
- ¹⁰J. O. Haerter, M. R. Peterson, and B. S. Shastry, *Phys. Rev. Lett.* **97**, 226402 (2006).
- ¹¹K. Kuroki and R. Arita, *J. Phys. Soc. Jpn.* **76**, 083707 (2007).
- ¹²C. A. Marianetti and G. Kotliar, *Phys. Rev. Lett.* **98**, 176405 (2007).
- ¹³F. Lechermann, *Phys. Rev. Lett.* **102**, 046403 (2009).
- ¹⁴G. Khaliullin and J. Chaloupka, *Phys. Rev. B* **77**, 104532 (2008).
- ¹⁵G. Baskaran, *Phys. Rev. Lett.* **91**, 097003 (2003).
- ¹⁶B. Kumar and B. S. Shastry, *Phys. Rev. B* **68**, 104508 (2003).
- ¹⁷Q.-H. Wang, D.-H. Lee, and P. A. Lee, *Phys. Rev. B* **69**, 092504 (2004).
- ¹⁸M. Z. Hasan *et al.*, *Phys. Rev. Lett.* **92**, 246402 (2004).
- ¹⁹D. Qian, L. Wray, D. Hsieh, L. Viciu, R. J. Cava, J. L. Luo, D. Wu, N. L. Wang, and M. Z. Hasan, *Phys. Rev. Lett.* **97**, 186405 (2006).
- ²⁰S. Zhou, M. Gao, H. Ding, P. A. Lee, and Z. Wang, *Phys. Rev. Lett.* **94**, 206401 (2005).
- ²¹K. Wu, Z. Y. Weng, and J. Zaanen (unpublished).
- ²²R. Ray, A. Ghoshray, K. Ghoshray, and S. Nakamura, *Phys. Rev. B* **59**, 9454 (1999).
- ²³T. Motohashi, R. Ueda, E. Naujalis, T. Tojo, I. Terasaki, T. Atake, M. Karppinen, and H. Yamauchi, *Phys. Rev. B* **67**, 064406 (2003).
- ²⁴D. J. Singh, *Phys. Rev. B* **60**, 13397 (2000).
- ²⁵G. Beni, *Phys. Rev. B* **10**, 2186 (1974).
- ²⁶P. M. Chaikin and G. Beni, *Phys. Rev. B* **13**, 647 (1976).
- ²⁷Here μ_s is defined with taking the LLL energy $E_0 = 0$ such that $\mu_s(T = 0) = 0$.
- ²⁸R. B. Laughlin, *Phys. Rev. Lett.* **60**, 2677 (1988).
- ²⁹A. L. Fetter, C. B. Hanna, and R. B. Laughlin, *Phys. Rev. B* **39**, 9679 (1989).
- ³⁰Y. H. Chen, F. Wilczek, E. Witten, and B. I. Halperin, *Int. J. Mod. Phys. B* **3**, 1001 (1989).
- ³¹Z.-C. Gu and Z.-Y. Weng, *Phys. Rev. B* **76**, 024501 (2007).
- ³²M. R. Peterson, B. S. Shastry, and J. O. Haerter, *Phys. Rev. B* **76**, 165118 (2007).
- ³³I. R. Mukhamedshin, H. Alloul, G. Collin, and N. Blanchard, *Phys. Rev. Lett.* **93**, 167601 (2004).
- ³⁴H. Alloul *et al.*, *Europhys. Lett.* **82**, 17002 (2008).
- ³⁵H. Alloul *et al.*, *Europhys. Lett.* **85**, 47006 (2009).
- ³⁶T. F. Schulze *et al.*, *Phys. Rev. B* **78**, 205101 (2008).
- ³⁷Y. Okamoto, A. Nishio, and Z. Hiroi, *Phys. Rev. B* **81**, 121102 (2010).
- ³⁸A. T. Boothroyd, R. Coldea, D. A. Tennant, D. Prabhakaran, L. M. Helme, and C. D. Frost, *Phys. Rev. Lett.* **92**, 197201 (2004).
- ³⁹Y.-S. Li *et al.*, *Phys. Rev. Lett.* **93**, 056401 (2004).